Figure S1

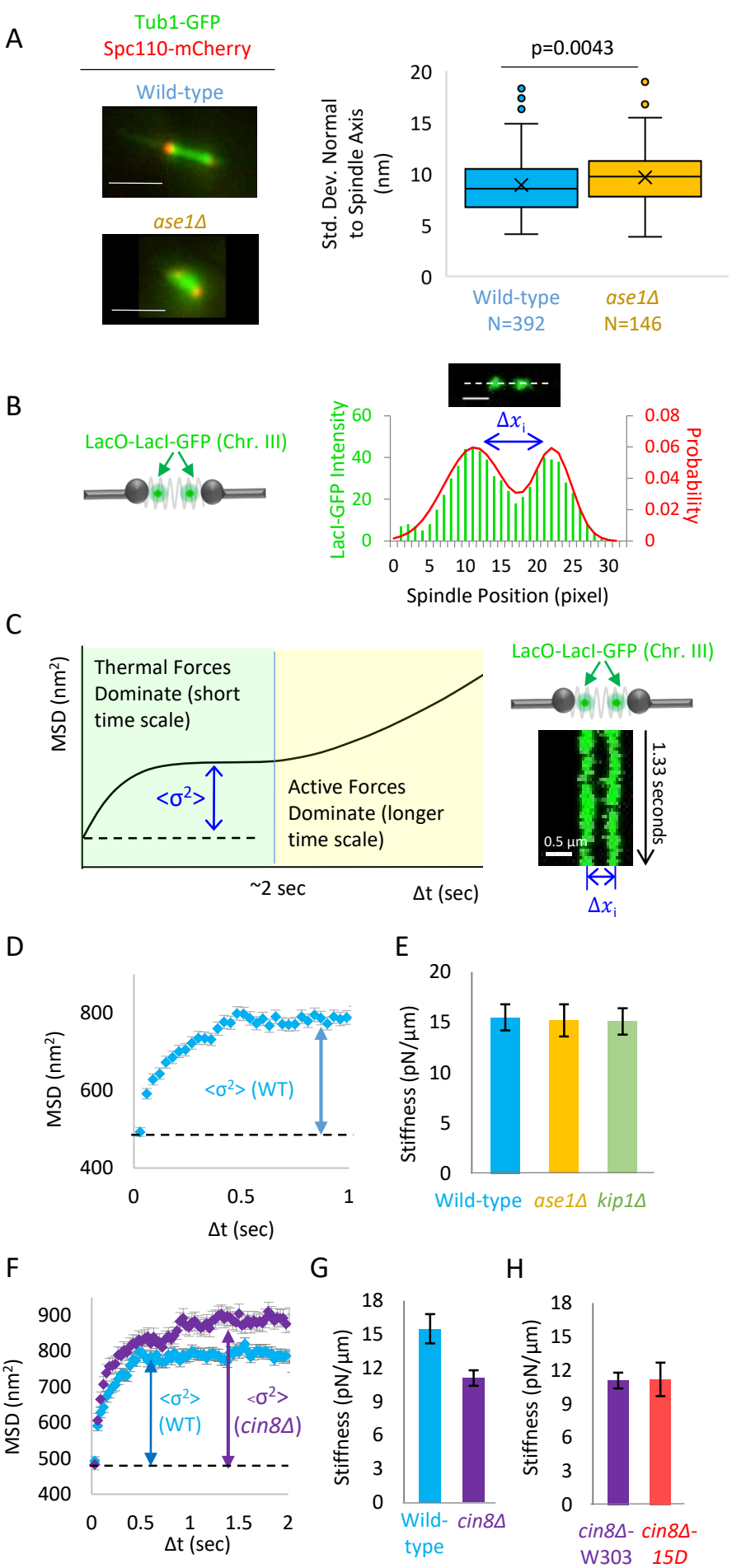
A
Tub1-GFP
Spc110-mCherry
Wild-type
ase1Δ
p=0.0043
Std. Dev. Normal to Spindle Axis (nm)
Wild-type N=392
ase1Δ N=146
B
LacO-LacI-GFP (Chr. III)
LacI-GFP Intensity
Probability
Δx_i
Spindle Position (pixel)
C
Thermal Forces Dominate (short time scale)
Active Forces Dominate (longer time scale)
MSD (nm²)
<σ²>
~2 sec
Δt (sec)
LacO-LacI-GFP (Chr. III)
1.33 seconds
0.5 μm
Δx_i
D
MSD (nm²)
<σ²> (WT)
Δt (sec)
E
Stiffness (pN/μm)
Wild-type
ase1Δ
kip1Δ
F
MSD (nm²)
<σ²> (WT)
<σ²> (cin8Δ)
Δt (sec)
G
Stiffness (pN/μm)
Wild-type
cin8Δ
H
Stiffness (pN/μm)
cin8Δ-W303
cin8Δ-15D

Figure S1, Relates to Figure 1: Estimation of tension in the *S. cerevisiae* mitotic spindle at metaphase. (A) Left: Typical images of wild-type and *ase1Δ* cells (Green, Tub1-GFP, red, SPC110-mCherry; scale bar 1000 nm). Right: spindle width as estimated by fitting the standard deviation of a Gaussian distribution perpendicular to the spindle axis for Tub1-GFP fluorescence. *ase1Δ* spindles are wider than wild-type cell spindles (t = -2.87, p=0.0043). (B) Left: To estimate inter-kinetochore spring tension, a LacI-GFP fusion was localized to a tandem array of 33 lacO repeats inserted 1.1 kb 3' to CEN3. Right: Representation of fluorescence intensity of the lacO-lacI-GFP centromeric labels along the spindle axis as a histogram (green bars), and subsequent Gaussian fitting to accurately determine the center of each spot (red line)). To estimate tension, the distance between the two spots is determined, and designated as Δx_i. (C) Left: Mean squared displacement (MSD) is used to describe the variance in position between the two sister centromere lacO-lacI-GFP spots over time. At short time scales (left, green), this variability occurs as a result of thermal forces, and the MSD values reflect constrained diffusion. This is the time scale in which stiffness measurements are made. At longer time scales (right, yellow), active forces dominate, and so variability measurements were not collected in this regime. Right: Representative kymograph of lacO-lacI-GFP spots over time, using fast time-lapse imaging. Kymograph shows 40 frames imaged at 30 frames/sec. (D) Mean squared displacement (MSD) vs time step size curve for wild type *S. cerevisiae* cells (blue arrow shows calculated $<\sigma^2>$ value). (E) Comparison of spring constants for wild-type, *kip1Δ*, *ase1Δ* cells. (F) MSD vs time-step size curves comparing wild type (blue) with the *cin8Δ* mutant (purple). (blue and purple arrows show calculated $<\sigma^2>$ values). (G) Quantification of the spring constant in *cin8Δ* mutant as compared to wild-type cells. (H) Comparison of spring constants in *cin8Δ* mutants from two different strain backgrounds. All panels: error bars=SEM.

Figure S2

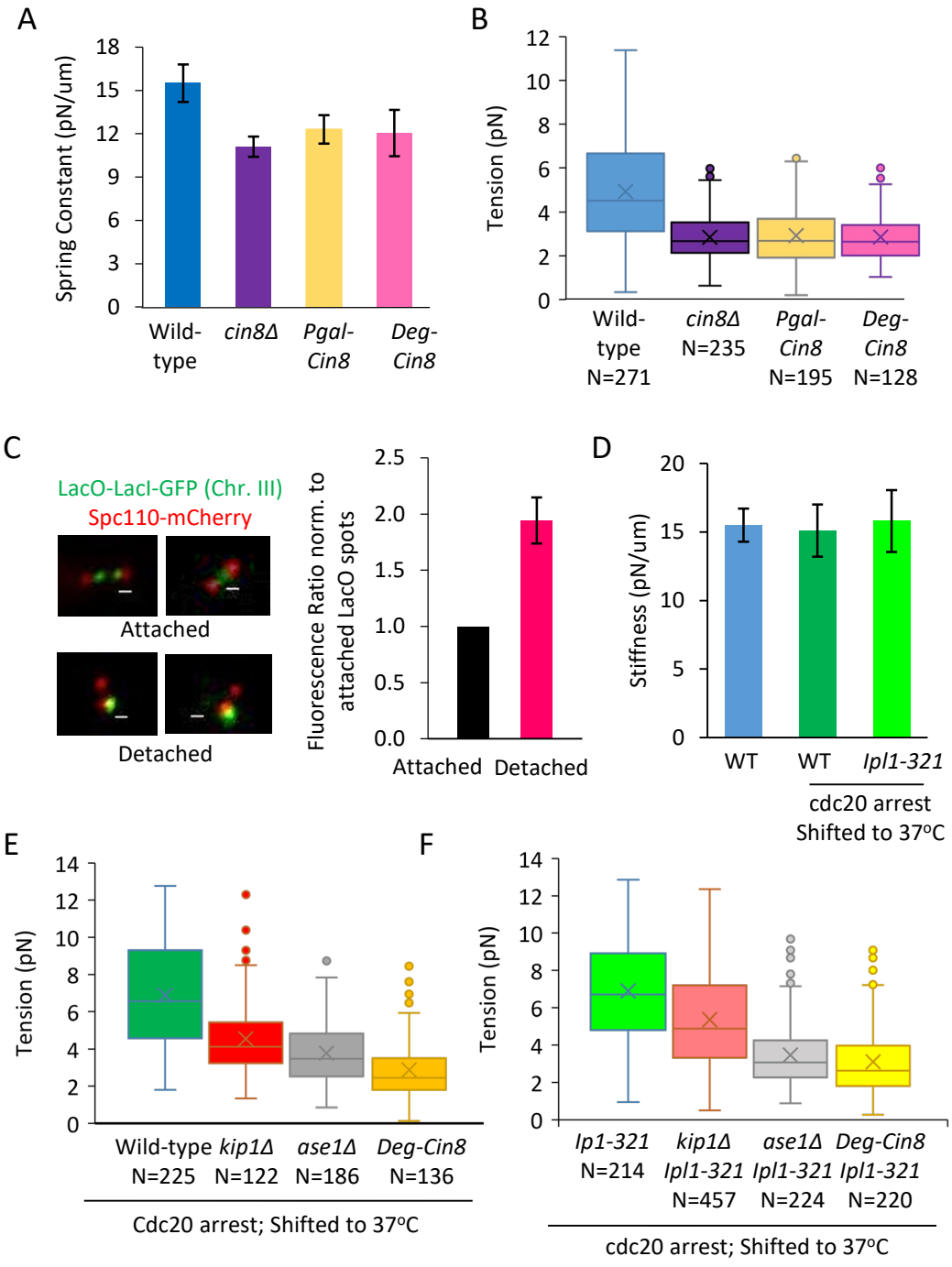
A
Spring Constant (pN/um)
18
15
12
9
6
3
0
Wild-type
cin8Δ
Pgal-Cin8
Deg-Cin8
B
Tension (pN)
12
10
8
6
4
2
0
Wild-type N=271
cin8Δ N=235
Pgal-Cin8 N=195
Deg-Cin8 N=128
C
LacO-LacI-GFP (Chr. III)
Spc110-mCherry
Attached
Detached
Fluorescence Ratio norm. to attached LacO spots
2.5
2.0
1.5
1.0
0.5
0.0
Attached
Detached
D
Stiffness (pN/um)
20
15
10
5
0
WT
WT
Ipl1-321
cdc20 arrest
Shifted to 37°C
E
Tension (pN)
14
12
10
8
6
4
2
0
Wild-type N=225
kip1Δ N=122
ase1Δ N=186
Deg-Cin8 N=136
Cdc20 arrest; Shifted to 37°C
F
Tension (pN)
14
12
10
8
6
4
2
0
Ip1-321 N=214
kip1Δ Ipl1-321 N=457
ase1Δ Ipl1-321 N=224
Deg-Cin8 Ipl1-321 N=220
cdc20 arrest; Shifted to 37°C

Figure S2, Relates to Figure 2: Additional tension and detachment data. (A) Comparison of spring constants in Cin8 conditional mutants as compared to wild-type and *cin8Δ* cells. Pgal-cin8 cells were grown and imaged in glucose to repress Cin8 expression for comparison to Deg-Cin8. Deg-Cin8 cells were imaged with induction of Cin8 degradation. (B) Comparison of average tension magnitudes in wild-type, *cin8Δ* and Cin8 conditional knockout cells ($F_{2,554} = 0.25$, $p = 0.77$, *cin8Δ vs* Pgal-Cin8 *vs* deg-Cin8). (C) Measurement of lacO-lacI-GFP intensity in cells with separated lacO-lacI-GFP spots (kinetochores attached), and cells with a single diffraction-limited spots (one detached kinetochore) (scale bars 500 nm). (D) Comparison of spring constant between wild type asynchronous cells at metaphase, and cells arrested with Cdc20 depletion and shifted to 37 °C. (E) Quantification of tension in cells that were arrested with Cdc20 depletion and shifted to 37 °C ($F_{3,665} = 124.05$, $p<.0001$). (F) Quantification of tension in cells harboring the *ipl-321* allele, arrested with Cdc20 depletion and shifted to 37 °C ($F_{3,1151} = 139.43$, $p<.0001$).

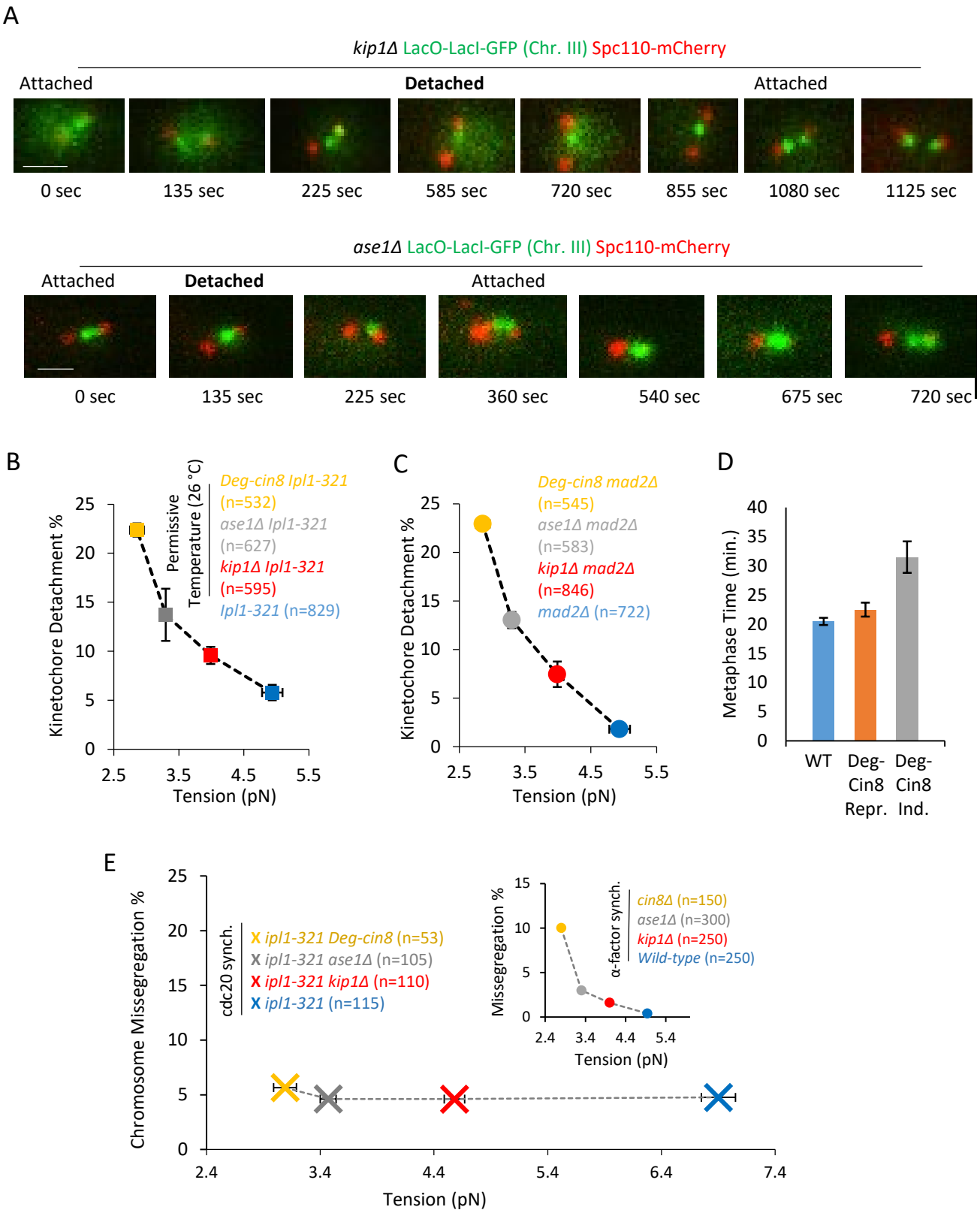
A
kip1Δ LacO-LacI-GFP (Chr. III) Spc110-mCherry
Attached
Detached
Attached
0 sec
135 sec
225 sec
585 sec
720 sec
855 sec
1080 sec
1125 sec
ase1Δ LacO-LacI-GFP (Chr. III) Spc110-mCherry
Attached
Detached
Attached
0 sec
135 sec
225 sec
360 sec
540 sec
675 sec
720 sec
B
Kinetochore Detachment %
Permissive Temperature (26 °C)
Tension (pN)
Deg-cin8 Ipl1-321 (n=532)
ase1Δ Ipl1-321 (n=627)
kip1Δ Ipl1-321 (n=595)
Ipl1-321 (n=829)
C
Kinetochore Detachment %
Tension (pN)
Deg-cin8 mad2Δ (n=545)
ase1Δ mad2Δ (n=583)
kip1Δ mad2Δ (n=846)
mad2Δ (n=722)
D
Metaphase Time (min.)
WT
Deg-Cin8 Repr.
Deg-Cin8 Ind.
E
Chromosome Missegregation %
Tension (pN)
cdc20 synch.
X ipl1-321 Deg-cin8 (n=53)
X ipl1-321 ase1Δ (n=105)
X ipl1-321 kip1Δ (n=110)
X ipl1-321 (n=115)
Missegregation %
α-factor synch.
cin8Δ (n=150)
ase1Δ (n=300)
kip1Δ (n=250)
Wild-type (n=250)
Tension (pN)

Figure S3, Relates to Figure 2: Additional detachment and mis-segregation data. (A) Images from time series in metaphase *kip1Δ* mutants (top) and *ase1Δ* mutants (bottom) demonstrating dynamic kinetochore attachments. (B) Dependence of detachments on magnitude of tension in cells harboring the ipl-321 allele, at permissive temperature (26 °C) ($z = -8.14$, $p<0.0001$, Cochran-Armitage trend test). (C) Dependence of detachments on magnitude of tension in *mad2Δ* mutant background cell lines ($z = -11.29$, $p<0.0001$, Cochran-Armitage trend test). (D) Comparison of metaphase time in the Degron-cin8 mutant under conditions of degron repression (orange) and degron induction (gray). (E) To test the prediction that the observed tension dependent chromosome mis-segregation gradient would be abrogated in the absence of Aurora B activity, we first arrested wild type and tension mutant cells that harbored the temperature-sensitive Aurora B allele *ipl1-321* in metaphase using Cdc20 under a repressible promoter. This was performed at the permissive temperature for *ipl1-321*, since inactivation of *ipl1-321* prior to metaphase could induce premature attachment errors which might confound our analysis. We then shifted the cells to the restrictive temperature for the *ipl-321* allele while cells were still in metaphase. Finally, we released cells from the cdc20 arrest, allowing them to complete metaphase and enter anaphase while at the restrictive temperature for *ipl1-321* allele, and assayed for chromosome mis-segregation as previously described. We observed an abrogation in the tension dependent chromosome mis-segregation gradient, consistent with our kinetochore detachment results (Fig. 2E). Inset: For reference the mis-segregation results in the absence of the ipl1-321 allele are shown, with data reproduced from Fig. 2D. All panels: error bars=SEM.

Figure S4

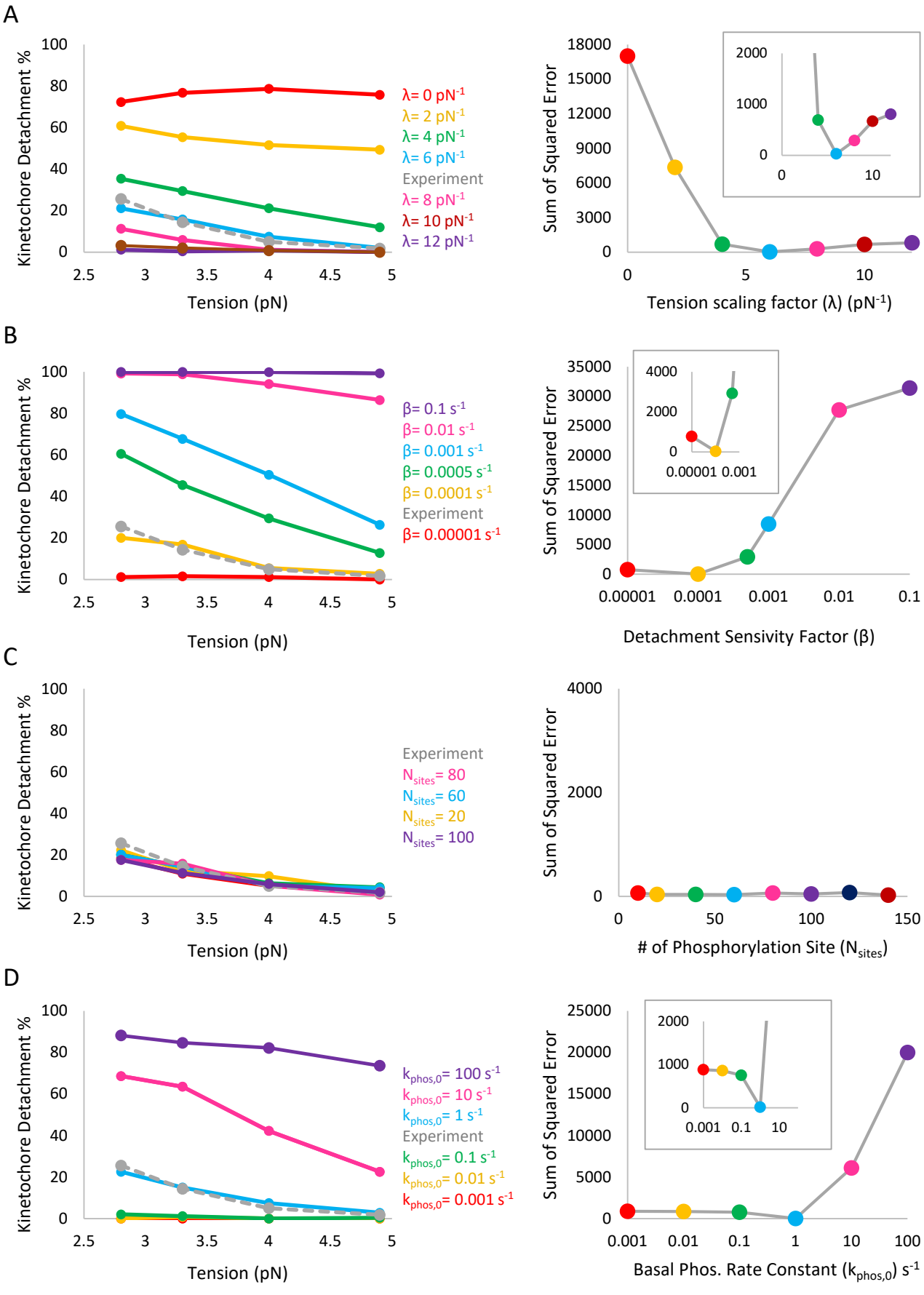
A
Kinetochore Detachment %
Tension (pN)
λ= 0 pN-1
λ= 2 pN-1
λ= 4 pN-1
λ= 6 pN-1
Experiment
λ= 8 pN-1
λ= 10 pN-1
λ= 12 pN-1
Sum of Squared Error
Tension scaling factor (λ) (pN-1)
B
β= 0.1 s-1
β= 0.01 s-1
β= 0.001 s-1
β= 0.0005 s-1
β= 0.0001 s-1
Experiment
β= 0.00001 s-1
Detachment Sensivity Factor (β)
C
Experiment
Nsites= 80
Nsites= 60
Nsites= 20
Nsites= 100
# of Phosphorylation Site (Nsites)
D
kphos,0= 100 s-1
kphos,0= 10 s-1
kphos,0= 1 s-1
Experiment
kphos,0= 0.1 s-1
kphos,0= 0.01 s-1
kphos,0= 0.001 s-1
Basal Phos. Rate Constant (kphos,0) s-1

Figure S4, Relates to Figure 4: Simulation parameter sensitivity analysis. (A) Sensitivity of simulation results to the tension scaling factor (λ). Left: Kinetochore detachment % vs tension for each parameter, experimental data shown in dotted grey line. Right: SSE (sum of squared errors) represents the summed error between simulation and experiment for kinetochore detachment % (see simulation methods). A smaller number indicates better fit. Inset shows rescaled y-axis for clarity. (B) Sensitivity of simulation results to the detachment scaling factor (β). Simulation results are sensitive to β for β>0.001. Left: Kinetochore detachment % vs tension for each parameter, experimental data shown in dotted grey line. Right: SSE (sum of squared errors) represents the summed error between simulation and experiment for kinetochore detachment % (note that x-axis is log to demonstrate results over 5 orders of magnitudes) (see simulation methods). A smaller number indicates better fit. Inset shows rescaled y-axis for clarity. (C) Sensitivity of simulation results to the total number of kinetochore phosphorylation sites (N_{sites}). Simulation results are insensitive to the parameter N_{sites}, likely because results are sensitive to the *fraction* of phosphorylated sites, and thus are insensitive to the absolute number of sites (N_{sites}) within a single kinetochore. Left: Kinetochore detachment % vs tension for each parameter, experimental data shown in dotted grey line. Right: SSE (sum of squared errors) represents the summed error between simulation and experiment for kinetochore detachment % (see simulation methods). A smaller number indicates better fit. (D) Sensitivity of simulation results to the basal (no tension) phosphorylation rate constant ($k_{phos,0}$). Simulation results are sensitive to $k_{phos,0}$, especially for values of $k_{phos,0} > 1\ s^{-1}$. Left: Kinetochore detachment % vs tension for each parameter, experimental data shown in dotted grey line. Right: SSE (sum of squared errors) represents the summed error between simulation and experiment for kinetochore detachment % (see simulation methods). A smaller number indicates better fit. Inset shows rescaled y-axis for clarity.

Figure S5

A

Combined MALDI spectrum

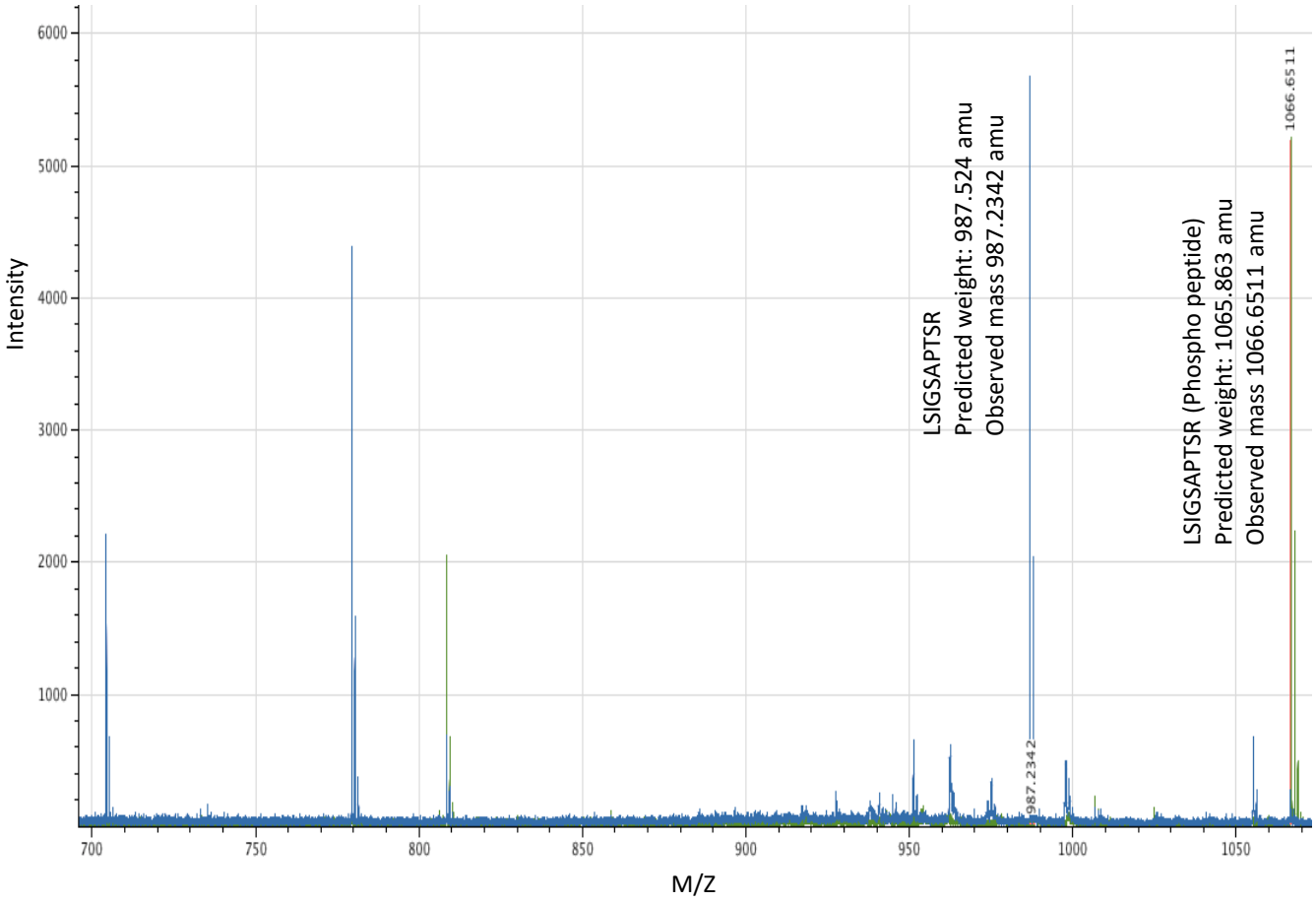

B

MS/MS Sequence

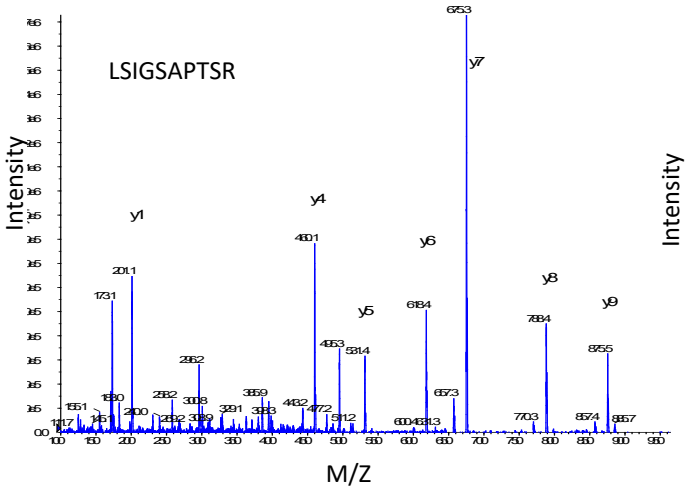

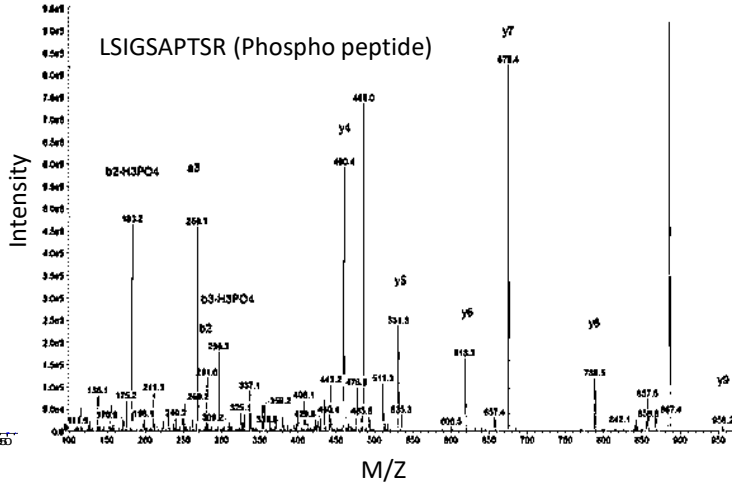

Figure S5, Relates to Figure 5: Mass Spectroscopy Data. (A) Combined Matrix Assisted Laser Desorption/Ionization (MALDI) spectra of crude synthetic peptide demonstrating mass to charge ratio (m/z) of 987.2342 (expected $[M+H]^+$ = 987.114) for the dephosphorylated Dam1 peptide LSIGSAPTSR and m/z of 1066.6511 (expected $[M+H]^+$ = 1067.034) for the phosphorylated Dam1 peptide L(Phospho-S)IGSAPTSR. Measurements were taken on a Bruker Autoflex MALDI mass spectrometer (Bremen, Germany) (B) Upon HPLC purification both peptides were verified using liquid chromatography-tandem mass spectrometry (LC MS/MS) with prominent peaks representative of the expected Y4, Y5, Y6, Y7, Y8, and Y9 species detected in both the dephosphorylated and phosphorylated LSIGSAPTSR peptides. Measurements were taken on a SCIEX 5500 Qtrap Triple Quadrupole Mass Spectrometer (Framingham, MA).